Lewis, S. C., King, A. D., Perkins-Kirkpatrick, S. E., & Mitchell, D. M. (2019). Regional hotspots of temperature extremes under 1.5°C and 2°C of global mean warming. *Weather and Climate Extremes*, *26*, [100233]. https://doi.org/10.1016/j.wace.2019.100233

Weather and Climate Extremes 26 (2019) 100233

Contents lists available at ScienceDirect

Weather and Climate Extremes

journal homepage: http://www.elsevier.com/locate/wace

Regional hotspots of temperature extremes under 1.5 °C and 2 °C of global mean warming

Sophie C. Lewis [a,*], Andrew D. King [b], Sarah E. Perkins-Kirkpatrick [c], Daniel M. Mitchell [d]

[a] School of Physical Environmental and Mathematical Sciences, University of New South Wales, Canberra, ACT, Australia
[b] School of Earth Sciences, The University of Melbourne, Parkville, Victoria, Australia
[c] Climate Change Research Centre, University of New South Wales, Sydney, UNSW, Australia
[d] School of Geographical Sciences, University of Bristol, Bristol, UK

A B S T R A C T

Local- and regional-scale heat extremes can increase at a significantly greater rate than global mean changes, presenting challenges for human health, infrastructure, industry and ecosystems. We examine changes in regional absolute temperature extremes for a suite of global regions under 1.5 °C and 2 °C of warming above pre-industrial levels, as described by the Paris Agreement. We focus on area-average values of observed monthly averages of daily maximum and minimum temperatures in 12 regions and calculate the most extreme monthly records observed. Next, using a large ensemble (HAPPI; Half a Degree Additional warming, Prognosis, and Projected Impacts) of decade-long simulations both of the present day and stabilised at these higher warming thresholds, we explore how changes in temperature extremes temperatures scale with global mean warming in these timeslice simulations. In the models, we focus on the 99th percentile values of monthly maximum temperatures and the 1st percentile of the monthly minimum temperatures. We define and identify hotspots of warming for various global mean warming levels, where projected changes in regional extremes are greater than global mean temperature changes. We identify overall hotspots of extremes, which are regions where the tail of the temperature distribution (above 99th percentile) warms at a faster rate than the rest of the temperature distribution in response to mean global warming increase. For monthly maximum temperatures, Central Europe, North Asia, West and East North America experience the greatest projected increases in extremes relative to means, and for monthly minimum temperatures, Central, West, East and North Asia, and East North America are identified as extremes hotspots. Although the scaling of increasing extremes with global mean temperatures is regionally variable, all regions benefit from the reduced severity of monthly maximum temperatures under lower global warming thresholds.

1. Introduction

As extreme weather and climate events pose significant risks to human and natural systems, understanding past changes and future projections of extremes is an important and active research area. Studies have adopted various approaches to understanding future extremes and provide valuable information about possible future changes in extremes typically of a magnitude that has already been observed. These approaches include, for example, i) quantifying changes in the characteristics of extremes attributable to specific forcings (e.g., King et al., 2017; Nangombe et al., 2018), ii) assessing changes in the frequency or duration of extremes in the future (e.g., Perkins, 2015), iii) process-based (dynamic and land-surface) understandings of changes (Zappa and Shepherd, 2017) and iv) determining the time in the future when current extremes can no longer be considered an outcome of natural climates (e.g., King et al., 2016).

Fewer studies to date have examined potential changes in the magnitude of future temperature extremes (i.e. those which are unprecedented in the historical climate) under enhanced anthropogenic global mean warming levels such as Paris Agreement levels. The 2015 Paris Agreement on Climate Change commits to '[h]olding the increase in the global average temperature to less than 2 °C above pre-industrial levels and to pursue efforts to limit the temperature increase to only 1.5 °C above pre-industrial levels, recognizing that this would significantly reduce the risks and impacts of climate change' (UNFCCC, 2016). Projections for Australia show unprecedented temperature extremes are simulated even under the Paris Agreement global mean warming targets, and do not necessarily scale with global mean warming, or with current observational record-breaking temperatures (Lewis et al., 2017).

Further studies have examined the relationship between regional temperatures and global mean temperatures (GMT) using pattern scaling approaches. Pattern scaling provides a means to assess future climate projections using spatial features of an externally forced change. Herger et al. (2015) explain that the "simplest traditional pattern scaling approach approximates future changes by the product of a time-evolving GMT change and a pattern that varies spatially but is constant over time,

* Corresponding author.
E-mail address: s.lewis@adfa.edu.au (S.C. Lewis).

https://doi.org/10.1016/j.wace.2019.100233
Received 27 March 2019; Received in revised form 8 September 2019; Accepted 4 October 2019
Available online 11 October 2019

scenario, and model characteristics." Some studies have shown that climate change signals in large-scale temperatures and precipitation patterns are linear as a function of global temperature (Tebaldi and Knutti, 2018). Pattern scaling approaches have been successful at emulating forced responses for varying degrees of global warming (King et al., 2018; Tebaldi and Arblaster, 2014) are consistent with model results showing changes in regional extreme temperatures tend to scale with GMT, independent of the emission scenario considered (Seneviratne et al., 2016). However, such scaling approaches are not universally applicable (King, 2019), and further analysis demonstrates that for extremes of temperature, this assumption of linearity may not hold in all locations (Lustenberger et al., 2014).

Understanding changes in the magnitude of future extremes with future GMT increases, in addition to previous work on changes in event frequency, is critical for determining the vulnerability of various systems to future climate change. On a global level, an assessment of changes in the severity of future extremes relative to global means has not been conducted, although previous work highlights that global temperature changes are much smaller than the expected changes in regional temperature extremes, making GMT a measure of limited use for overall climatic change (Seneviratne et al., 2016). In this current study, we look globally at how the magnitude of extreme temperatures events may differ from current conditions in the future by focusing on the Paris Agreement GMT levels. This globally-focused assessment is important, as exposure to future unfamiliar climates and extremes is regionally variable (Diffenbaugh et al., 2018). We also define and identify hotspots of future extreme temperatures (defined below), which are areas that demonstrate the strongest response in regional-scale extremes to global-scale mean warming of the land surface.

2. Data and analysis

2.1. Definitions of temperatures

We use a combination of observations and models to assess how the magnitude of temperatures extremes may change in the future. We focus this analysis on monthly, rather than daily or shorter duration, temperature extremes and examine in observations and models:

i) Tmax, which is the monthly average of daily maximum temperatures for all months
ii) Tmin, which is the monthly average of daily minimum temperatures in all months.

2.2. Observational data

For observations, we first compare values in two gridded observation-based products (Berkeley Earth Surface Temperature and CRU TS) that provide gridded monthly temperature data. The Berkley Earth (BEST) (Rohde and Coauthors, 2013) product merges temperature observations from multiple sources, providing a finer spatial resolution, and greater spatial and temporal coverage than CRU TS (Harris et al., 2014). We compare monthly temperature extremes in 25 land-dominated Intergovernmental Panel on Climate Change (IPCC, 2012) regions (excluding Antarctica, ANT) in the observed products, analyzing regions in which there is the closest agreement between products with the same spatial representation. For each IPCC region, area-average values of observed average monthly maximum temperatures are calculated and then a maximum record of regional values is determined (see Fig. 1a and b for BEST), rather than an area-average of gridbox maxima.

Regions are included for further analysis in BEST based on two criteria, 1) the difference in maximum recorded area-average Tmax values between BEST and CRU TS is less than 1 K and 2) less than half the standard deviation of temperature variability for that region. The 12 regions highlighted for further exploration in HAPPI models are listed in Table 1 and the similarity between observational data products can be seen in Fig. 1c for Tmax, and Fig. 1d for Tmin.

2.3. HAPPI data and evaluation

Projections of future temperature changes are determined from the HAPPI model dataset, which was designed for examining extreme events in simulated worlds that are 1.5 °C and 2 °C warmer than pre-industrial, in addition to the current (2006–2015) climate. Several prior studies have used transient, rather than timeslice, simulations (such as CMIP5) to examine facets of extremes although the difficulties of using such model frameworks have also been noted, including from the scenario

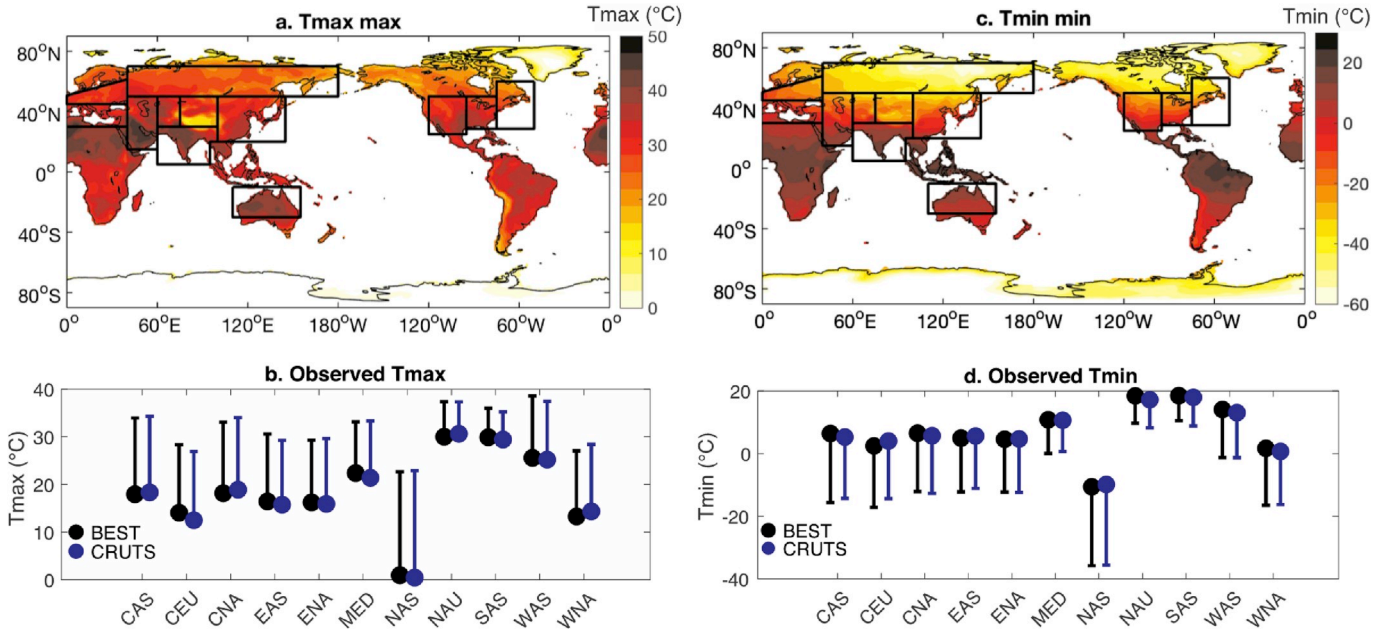

Fig. 1. (a) Observed record monthly Tmax values (°C) from BEST and boundaries of the regions analysed here. (b) Comparison of mean (circles) and record daily Tmax values (°C) in BEST and CRUTS datasets. Panels (c) and (d) show equivalent for Tmin values (°C).

Table 1
Summary of regions considered in BEST and CRUTS observational products and HAPPI data.

High observational agreement	High model-observational agreement	Regions analysed	Regions analysed (full name)
ALA	CAS	CAS	Central Asia
AMZ	CEU	CEU	Central Europe
CAM	CGI	CNA	Central North America
CAS	CNA	EAS	East Asia
CEU	EAS	ENA	East North America
CNA	ENA	MED	South Europe/ Mediterranean
EAF	MED	NAS	North Asia
EAS	NAS	NAU	North Australia
ENA	NAU	SAS	South Asia
MED	SAS	SEA	Southeast Asia
NAS	SEA	SSA	Southeastern South America
NAU	SSA	TIB	Tiberan Plateau
SAF	TIB	WAS	West Asia
SAS	WAS	WNA	West North America
SEA	WNA		
TIB			
WAF			
WAS			
WNA			
WSA			

dependence of warming (Wang et al., 2017). Mitchell et al. (2016) point out that there is a large spread in timing for when transient CMIP models cross global mean warming thresholds and the relative importance of difference forcings at these disparate times. Simulations like HAPPI that are tailored to 1.5 °C and 2.0 °C targets provide an avenue for exploring extremes and return times under stabilised climates (Mitchell and Co-authors, 2017). For a comprehensive discussion of the different methods used in producing projections of extremes see James et al. (2017).

Participating HAPPI models (NorESM1, ECHAM63LR, CanAM4, Cam4-degree and MIROC5) contribute large atmosphere-only ensembles for three decade-length timeslices, including 2006–2015 (historical or $HAPPI_{2006\text{-}2015}$) and under 1.5 °C and 2 °C ($HAPPI_{1.5}$ and $HAPPI_2$) of warming. Realisations, or ensemble members, within an experiment differ in their initial weather state. Simulations of the current decade (2006–2015) are driven by observed sea surface temperatures (SSTs) and sea ice. Boundary conditions for $HAPPI_{1.5}$ ($HAPPI_2$) are calculated by adding the change between the decadal average of the modelled 2006–2015 period and the decadal average of the modelled 1.5 °C (2 °C) world over 2091–2 100 to the observed 2006–2015 SSTs. Changes are determined from the CMIP5 (Taylor et al., 2012) multi-model ensemble from the representative concentration pathway 2.6 (RCP2.6) $HAPPI_{1.5}$ and RCP4.5 for $HAPPI_2$. We use multiple realisations of HAPPI Tmax (monthly average of daily maximum temperatures) and Tmin (monthly average of daily minimum temperatures) data (Table 2). A minimum of 500 decade-long realisations was used for each experiment, providing at least 6000 months of temperature data. Regional area-mean Tmax and Tmin are calculated in each HAPPI realisation.

Model Tmax data are compared to observations to evaluate how well observed variability is simulated, in addition to how accurately the multi-model ensemble mean matches observed. Following Lewis et al. (2017), variability in observed temperatures is estimated using synthesised timeseries. Using a bootstrap resampling method; we generated 2000 timeseries of 80-year length, calculated a suite of standard deviations of observed temperature and obtained a spread of plausible observed standard deviations, based on the BEST data. In this calculation, we have not removed an estimate of any trend over this period, and hence a larger variability in observed temperature may occur. However, the probability density functions (PDFs) of simulated Tmax and Tmin values in $HAPPI_{2006\text{-}2015}$ are somewhat broader than observed in many regions (Supplementary Figs. 1a and b and Fig. 2a and b).

This larger simulated variability may indicate that the substantially larger sample size available in model data captures a broader range of temperatures, and hence greater variances. It is also possible that discrepancies in simulated and observed temperature distributions relate to observational uncertainties and spatial inhomogeneities in data collection (see Alexander and Coauthors, 2006). Alternatively, this may demonstrate key biases in capturing observed means and variability in AMIP runs may result from errors in model sensitivity to surface temperature forcings. Previous analyses of temperatures in model simulations demonstrate a sensitivity in simulated climates to modelling approach. For example, projected extreme temperatures may be systematically biased towards high temperatures in SST-driven simulations compared to fully coupled runs (Fischer et al., 2018). Further studies, however, advocate for the use of SST-driven simulations for assessing regional climate projections over land (He and Soden, 2016).

Due to these potential biases in SST-driven model runs, we consider only regions in which observed temperature characteristics are accurately simulated. We find 12 regions (CAS; CEU; CNA; EAS; ENA; MED; NAS; NAU; SAS; SSA; WAS; WNA as outlined in Table 1) in which simulated variability falls within the observed bootstrapped range and there is consistency in maximum recorded area-average Tmax in observed products. In addition to focusing on these 12 best performing regions, we use HAPPI data in combination with observed data as a constraint on simulated extremes (discussed in section 2.3). While a greater coverage of regions would be ideal for examining future

Table 2
Summary of models and realisations analysed.

model	Number of realisations		
	All-Hist	1.5	2
NorESM-1	135	125	125
CanAM4	100	100	100
Cam4-2°	520	500	120
ECHAM6-3-LR	100	100	100

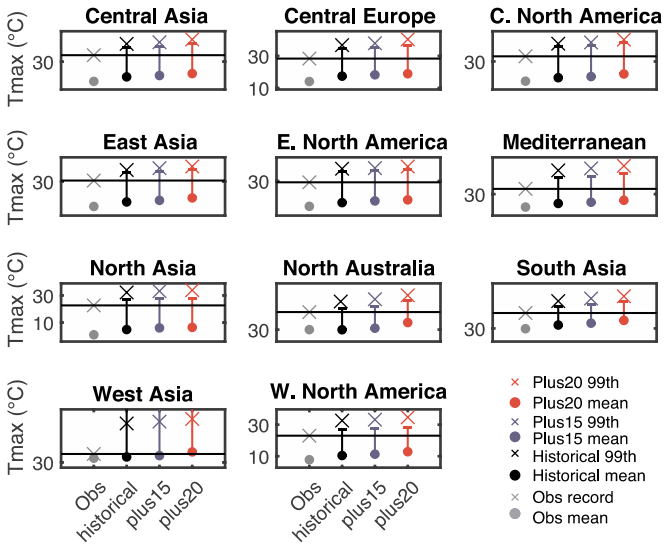

Fig. 2. Extreme monthly Tmax values (°C) in observations (grey), $HAPPI_{2006\text{-}2015}$ (black), $HAPPI_{1.5}$ (blue) and $HAPPI_2$ (red) for each analysed region. For observations, the plot circles represent observed mean values and crosses the recorded maximum. For HAPPI, the circles show ensemble mean values across all realisations, and crosses the ensemble 99th percentile values. The vertical lines for HAPPI show the observed constraints ($HAPPI_{1.5/Obs}$ and $HAPPI_{2/Obs}$). HAPPI values have been bias corrected using the observed mean and historical ensemble mean values.

extremes, we preference analysis of regions where models perform best compared with observed. We also note that the regions examined here provide coverage over many global areas (see Fig. 1a) and hence the potential for insight across a variety of areas. We also note that the regions examined here provide coverage over a diversity of areas across the globe (see Fig. 1a) and hence the potential for insight across a variety of climates. We also limit our analysis to monthly Tmax and Tmin, rather than daily temperatures, which demonstrate notable warm tail biases in many regions compared to observed (Supplementary Figs. 2a and b).

2.4. Defining future extremes and warming hotspots

Prior to calculating temperature values in HAPPI we apply a simple bias correction based on the differential between regional average Tmax values observed over 2006–2015 and the $HAPPI_{2006\text{-}2015}$ ensemble mean value (historical). This correction is applied to HAPPI simulated mean and extreme values for all experiments. Next Tmax and Tmin temperatures in HAPPI experiments are investigated using several analytical steps.

First, we calculate the ensemble mean Tmax values for each HAPPI experiment for each region for various percentile levels. Percentile values are calculated by first fitting a generalised extreme value (GEV) distribution to the Tmax timeseries for each realisation and calculating percentile values in the fitted distribution. Distributions are fitted to the raw time series rather than seasonally-corrected anomalies. Values are calculated for 99th, 95th, 90th, 75th percentiles in $HAPPI_{1.5}$ and $HAPPI_2$ (e.g., $HAPPI_{1.5/99}$; $HAPPI_{2/99}$) in each realisation and an ensemble mean value calculated. Equivalently, we calculate 1st, 5th, 10th and 25th percentile Tmin values (e.g., $HAPPI_{1.5/1}$; $HAPPI_{2/1}$) from the Tmin timeseries. A range of percentile values are provided for comparison, although we focus primarily on 99th Tmax and 1st Tmin values. This measure ideally provides a comparatively conservative estimate of future extreme temperatures, with this value, for example, exceeded every 1-in-100 months under 1.5 °C level of global mean warming for $HAPPI_{1.5/99}$ $HAPPI_{2/99}$. As with (Wehrli et al., 2018), we also find values are robust to statistical model fitted, models and number of realisations included, including if percentile values are calculated directly from timeseries without fitting a GEV distribution. We also note that the percentile values used are not all inherently extreme, but are rather selected to provide information on changes across a large part of the temperature distribution.

Second, we compare simulated warming across regions. We begin by applying an observational constraint to the magnitude of future simulated extremes, with the constraint based on observed and simulated standard deviations. Following Lewis et al. (2017), we use a two-step process wherein we:

i) determine the largest temperature range in the observations (extending from observed average to observed record), by calculating the number of observed standard deviations above the 2006–2015 mean ($N\sigma_{Obsmax}$) that defines the observed maximum anomaly value (Obs_{max})
ii) determine the equivalent range of extreme values in $HAPPI_{1.5}$ and $HAPPI_2$, based on the ensemble mean (μ) and standard deviation ($\sigma_{HAPPI1.5}$; σ_{HAPPI2}) in the 1.5 °C and 2 °C degree futures and the observed anomaly

$$HAPPI_{1.5/Obs} = \mu_{HAPPI1.5} + (N\sigma_{Obs\_max} * \sigma_{HAPPI1.5}) \quad 1a$$

$$HAPPI_{2/Obs} = \mu_{HAPPI2} + (N\sigma_{Obs\_max} * \sigma_{HAPPI2}) \quad 1b$$

Using these calculated projected temperature extremes, we identify regions as hotspots for each warming threshold (1.5 °C and 2 °C). These hotspots are regions where scaling of extremes ($HAPPI_{1.5/99}$ and $HAPPI_{2/99}$) between the two future warming scenarios is greater than the rate of change in global land surface mean temperature (GLMT).

$$\frac{\Delta HAPPI_{1.5/99}}{\Delta HAPPI_{1.5/GLMT}} > 1 \quad 2a$$

$$\frac{\Delta HAPPI_{2/99}}{\Delta HAPPI_{2/GLMT}} > 1 \quad 2b$$

Third, we identify overall hotspots of future warming of extremes, where the increase in 99th percentile extreme temperatures exceeds the increase in 95th percentile temperatures. The designation of regions as future hotspots of Tmax or Tmin warming can be summarised as identifying regions where the tail of the temperature distribution expands more between 1.5 °C and 2 °C of warming, than between historical (2006–2015) mean warming and 1.5 °C. To identify extremes hotspots, we:

i) calculate $\Delta HAPPI_{99}$, the difference in 99th percentile values between the 2 °C ($HAPPI_{2/99}$) and 1.5 °C ($HAPPI_{1.5/99}$) simulations
ii) calculate $\Delta HAPPI_{95}$, the difference in 95th percentile values between the 2 °C ($HAPPI_{2/95}$) and 1.5 °C ($HAPPI_{1.5/95}$) simulations
iii) categorise regions as maximum temperature hotspots where changes in extreme temperature values are greater at 2 °C of warming than 1.5 °C, fulfilling the condition that:

$$\frac{\Delta HAPPI_{99}}{\Delta HAPPI_{95}} > 1 \quad 3a$$

The equivalent minimum temperature extremes hotspots occur where

$$\frac{\Delta HAPPI_{1}}{\Delta HAPPI_{5}} > 1 \quad 3b$$

These steps identify hotspots regions where extremes warm faster than GMT (assuming that global mean warming in the historical simulations from 2006 to 2015 is 1 °C above pre-industrial (Haustein et al., 2017)).

In summary, these analytical approaches provide various assessments of how extreme Tmax and Tmin in various regions change with background global land surface warming, including how regional extremes scale with GLMT and how the tails of the regional temperature distributions change with warming.

3. Results

The simulated regional-average 99th percentile Tmax values exceed the current observed record in all instances for $HAPPI_{1.5}$ and $HAPPI_2$ (Fig. 2). In all regions except for WAS (West Asia) the observed constraint value, determined as the number of anomalous standard deviations above the mean defining the current observed record, is lower than $HAPPI_{1.5/99}$ or $HAPPI_{2/99}$. Conversely, for WAS, the observed constraint is larger than the 99th percentile simulated, indicating that temperatures at least as large as the $HAPPI_{1.5/99}$ or $HAPPI_{2/99}$ values should be expected to occur under these warming thresholds based on both observed and simulated characteristics of temperatures for this region. In all other analysed regions, the observed constraint is larger than $HAPPI_{1.5/99}$ and $HAPPI_{2/99}$ values, and these values are used hereafter to described future extremes under these global mean warming levels.

For Tmin, projected changes relative to observed records are less consistent across regions (Fig. 3). In certain regions, projected temperatures are cooler than those encountered to date (e.g. North and South Asia, North Australia and Eastern North America). These regions may incur other climatological changes that result in less warming in cold extremes than elsewhere, possibly due to precipitation trends or the occurrence of cold outbreaks. There is also a larger range of Tmin values for the WAS region determined through model estimates than indicated by observed values, suggesting that the SSTs imposed in the model do not provide a sufficient constraint on WAS temperatures. The WAS

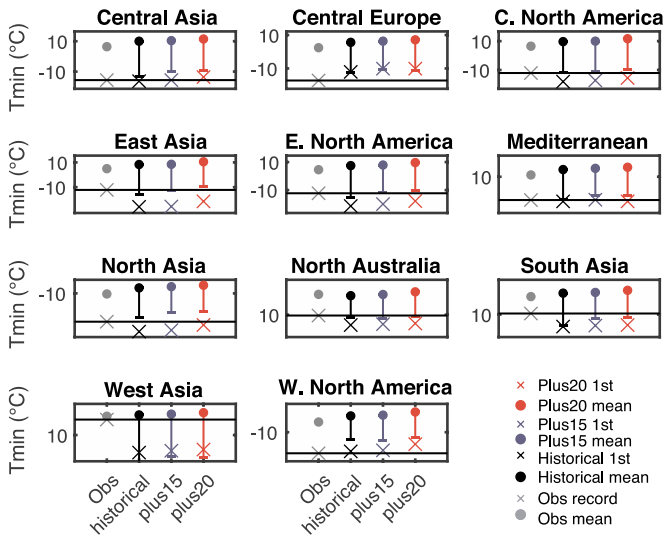

Fig. 3. As for Fig. 2, but showing Tmin values (°C) in $HAPPI_{2006\text{-}2015}$ (black), $HAPPI_{1.5}$ (blue) and $HAPPI_2$ (red) for each analysed region (crosses show ensemble 1st percentile values).

region, including the Arabian Peninsula, is subjected to strong westerly wind flow, meaning that the SST conditions imposed act as less of a constraint in this region compared to regions with ocean-dominated flow. For WAS, it is also possible that conditions occurring during 2006–2015 may not be sufficiently representative of climatic variability.

We next explore how extreme temperatures scale with mean warming (Figs. 4 and 5). For each region, we determine the relationship between ensemble mean and 99th percentile Tmax values in order to assess whether changes in extreme values exceed changes in regional mean Tmax values, as well as the 95th, 90th and 75th percentile values. The same approach is applied to the ensemble mean and 1st, 5th, 10th and 25th percentile Tmin values (Fig. 5). In many of the analysed regions shown in Fig. 4, $HAPPI_{1.5}$ or $HAPPI_2$ values fall above the identity line wherein mean and extreme values increase comparably. The specific regions vary depending on the percentile value examined. Similarly, several regions demonstrate warming of Tmin (1st percentile) at a rate exceeding increases in monthly means of daily mean temperatures (Fig. 5).

Regions in which extreme-global mean land surface scaling exceeds 1:1 (where increases in extremes are greater than mean values) are designated hotspots and summarised in Table 3. These regions are highlighted by hatching for Tmax in Fig. 6 and Tmin in Fig. 7, and are notably different for the Tmax and Tmin parameters. At 1.5 °C of global mean warming, Tmax warming hotspots occur for Central Asia, East Asia, North Asia, South Asia, West Asia, Central Europe, Mediterranean and North Australia (Fig. 6a). At 2 °C of global mean warming, warming hotspots occur for East Asia, South Asia, Central Asia, Central Europe, Mediterranean, North Australia, Central North America and Eastern North America (Fig. 6b). For Tmin, 1.5 °C hotspot regions are Central Europe, West and North Asia, and Western and Central North America (Figs. 7a) and 2 °C hotspot regions are Central Europe, West, Central, South and North Asia, and Western, Central and Eastern North America (Fig. 7b). Central Europe is identified as a hotspot of warming for all warming levels and temperature variables and is discussed in further detail in section 4).

These Tmax extreme-mean relationships are shown in greater detail (see Fig. 8) for the Central Europe (CEU) and Mediterranean (MED) regions, which are hotspots at both warming threshold levels. In both regions there are clear increases in extreme Tmax values above the global mean land surface warming for both 1.5 °C and 2 °C of global mean warming. The increase in Tmax 99th percentile values in these regions is over twice the increase in global mean land surface warming. While these regions demonstrate simulated warming of Tmax extremes occurring more than twice the rate of global mean surface temperature changes, ascertaining the absolute value of extreme temperatures under these warming scenarios remains difficult due to potential biases in models and uncertainties in warming responses. Although HAPPI data

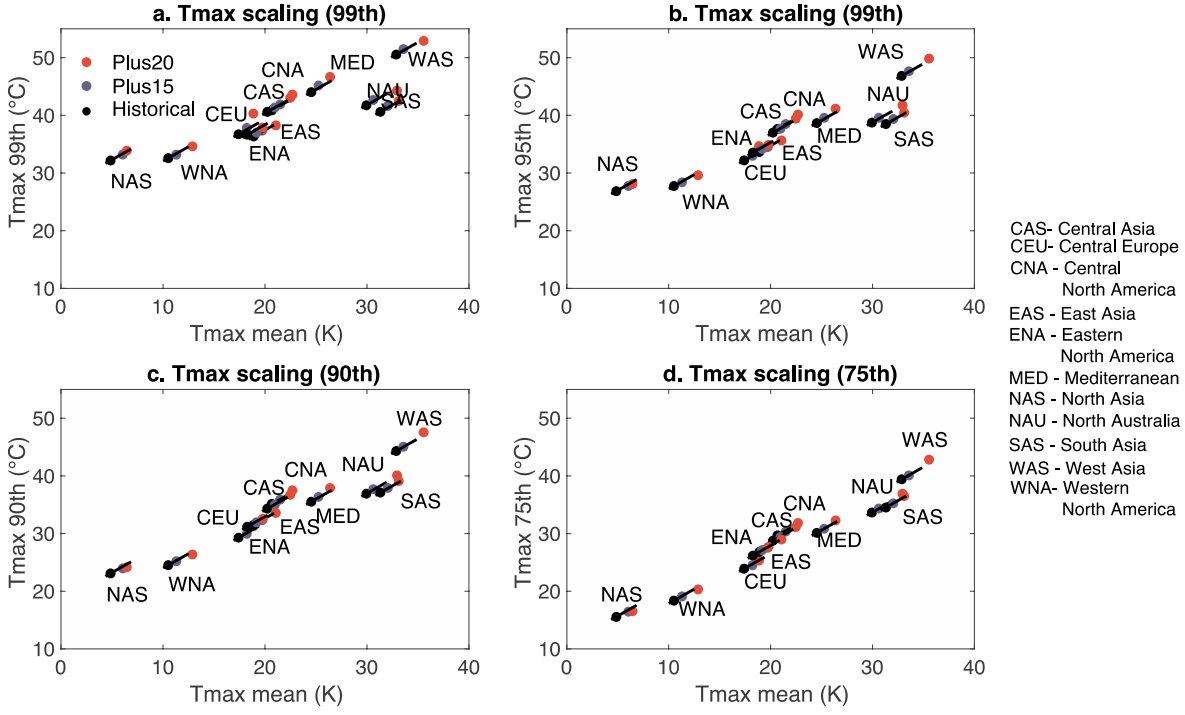

Fig. 4. HAPPI ensemble Tmax mean and 99th/95th/90th and 75th percentile values for each labelled region for each experiment ($HAPPI_{2006\text{-}2015}$ in black; $HAPPI1_{.5}$ in blue; $HAPPI_2$ in red). Scaling lines are shown for each region, demonstrating relationship if percentile values increased at same rate as mean. (For interpretation of the references to colour in this figure legend, the reader is referred to the Web version of this article.)

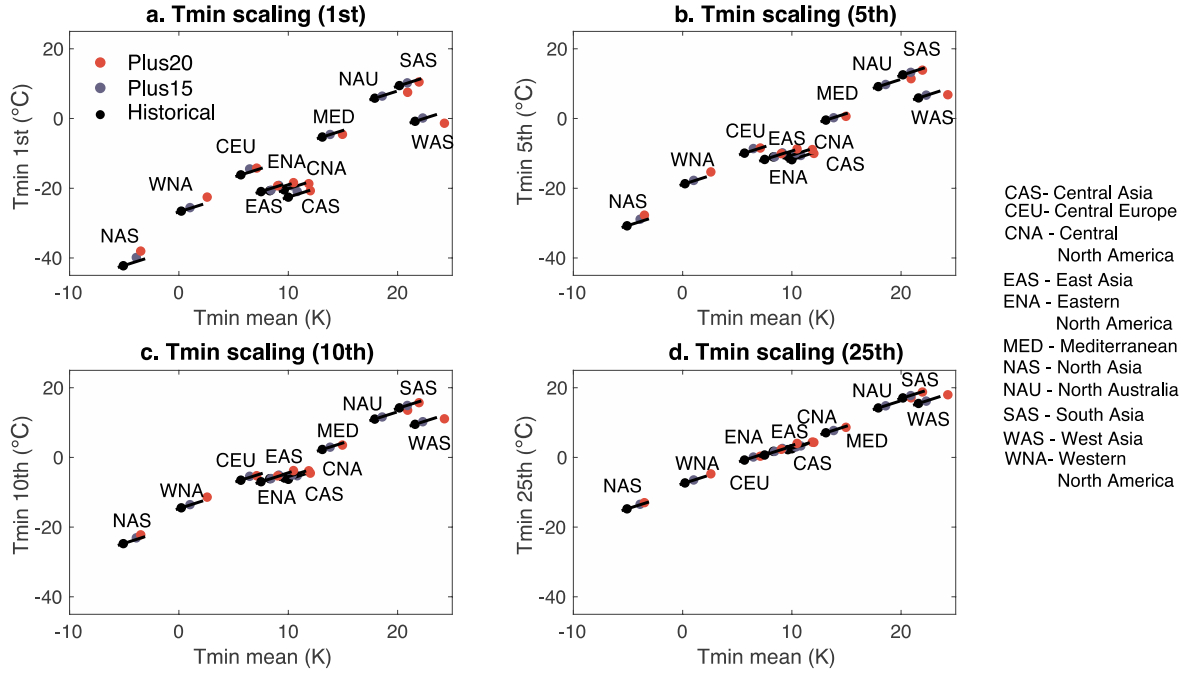

Fig. 5. HAPPI ensemble Tmin mean and 1st/5th/10th and 25th percentile values for each labelled region for each experiment ($HAPPI_{2006\text{-}2015}$ in black; $HAPPI1_{.5}$ in blue; $HAPPI_2$ in red). Scaling lines are shown for each region, demonstrating relationship if percentile values increased at same rate as mean. (For interpretation of the references to colour in this figure legend, the reader is referred to the Web version of this article.)

Table 3
Summary of hotspots of warming for Tmax and Tmin at 1.5 °C and 2 °C of warming (where regional extremes increase more rapidly than land surface mean temperatures) and extremes hotspots (where the tails of the temperature distributions expand under future warming).

		Hotspot regions
Tmax	1.5	CAS; EAS; NAS; SAS; WAS; CEU; MED; NAU
	2	EAS; SAS; CAS; CEU; MED; NAU; CAN; ENA
	Extremes	CEU; NAS; WNA; ENA
Tmin	1.5	CEU; WAS; NAS; WNA; CNA
	2	CEU; CAS; SAS; NAS; CNA; ENA
	Extremes	CAS; WAS: EAS; NAS; ENA

can be evaluated against observations for the recent period (2006–2015) to determine potential biases in mean model or variability, assessing the validity of $HAPP_{1.5}$ and $HAPPI_2$ simulations is harder.

In order to assess absolute temperature extreme values for these regions, we impose a further observational adjustment. We apply the observationally constrained simulated extreme values ($N\sigma_{Obs\_max}$ * $\sigma_{HAPPI1.5}$) to the recently observed regional mean temperatures (2006–2015) adjusted for future global mean warming levels. This aims to provide an observationally derived conservative estimate of future regional temperature extremes. Applying this approach to the highlighted hotspots regions gives temperature extremes up to 6 °C above existing records for just 1.5 °C of global mean warming in the Mediterranean, and a 1.8 °C increase in Tmax extremes between 1.5 °C and 2 °C of global mean warming. We discuss this very strong warming further later. For Tmin extremes we focus on WNA and CEU as hotspot regions of interest (Fig. 9). In both these regions, warming of Tmin extremes occur at a rate greater than warming of the global land surface, for both 1.5 °C and 2 °C of warming.

We summarise these results by identifying extremes hotspots of projected future warming (Fig. 10), where the tail of the temperature distribution expands with global mean warming levels in the HAPPI experiments. Hotspot regions for Tmax are CEU, NAS, WNA and ENA (Fig. 10a). For Tmin, hotspots are CAS, WAS, EAS, NAS and ENA

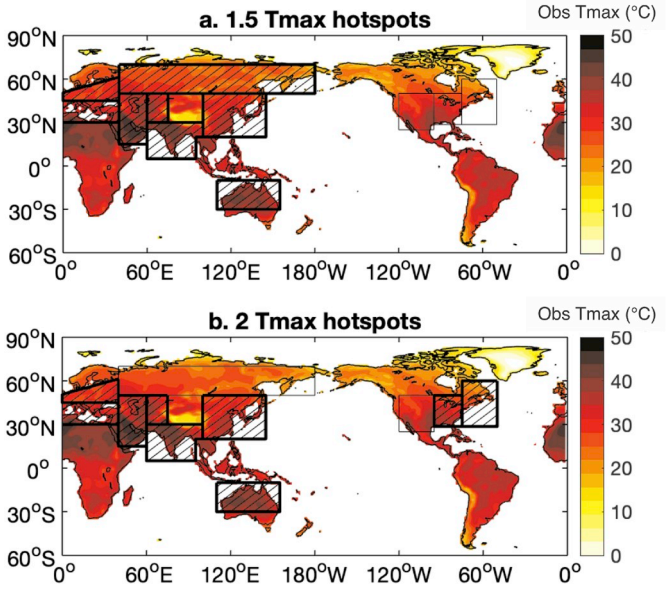

Fig. 6. Hotspots of future warming for 1.5 °C (a) and 2 °C (b) of warming against existing record observed Tmax values. Regions are highlighted by hatching where warming of extremes of monthly Tmax ($HAPPI_{1.5/99}$/$HAPPI_{2/99}$) global mean land surface warming.

(Fig. 10b). This summary of hotspots (Table 3) provides information about regions where the tail of the temperature distribution is most sensitive to warming between the two global mean thresholds.

4. Discussion

The results presented here are largely consistent with previous studies that have shown extreme local- or regional-scale temperatures increasing at a faster rate than mean temperature in some regions. By

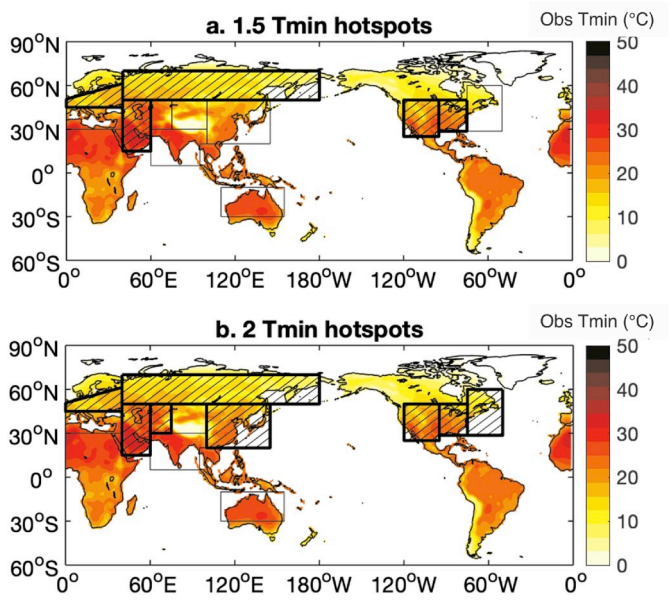

Fig. 7. Hotspots of future warming for 1.5 °C (a) and 2 °C (b) of warming against existing record observed Tmin values. Regions are highlighted by hatching where warming of extremes of monthly Tmin ($HAPPI_{1.5/99}$/$HAPPI_{2/99}$) exceeds global mean land surface warming.

exploring events of various durations in distinct model projects, studies have identified regions of accelerated warming (e.g. Coumou et al., 2013; Coumou and Robinson, 2013; Diffenbaugh and Giorgi, 2012). These highlighted examples typically use CMIP5 coupled models with transient simulations to assess changed in extremes relative to mean conditions for a suite of regions and temperature metrics, including for example warm seasons, rates of record-breaking and percentage of global land area experiencing extremes. Despite exploring extremes using diverse measures, prior studies generally demonstrate a consensus of larger increases in threshold exceeding extreme temperature events than of mean temperatures for many regions (Coumou and Robinson, 2013; Hansen et al., 2012).

This effect of disproportionate increases in regional-scale extreme temperatures is noted even in moving between levels of 1.5 °C and 2 °C of global mean warming. In one study examining Australian extremes, including seasonal temperatures, an increase of ~25% in the likelihood of record heat extremes was projected if warming of 2 °C rather than 1.5 °C occurred (King et al., 2017). Global warming of 2 °C results in substantially larger simulated changes in the probabilities of the extreme temperatures events over much of the land surface than for 1.5 °C of warming (Kharin et al., 2018). This effect is also reported for the contiguous USA (Karmalkar and Bradley, 2017) and for Europe (Dosio et al., 2017). More detailed studies of the relationships between local and regional temperature changes with global mean warming of 1.5 °C and 2 °C have been conducted (King et al., 2018). This study used transient CMIP5 climate simulation to evaluate how well simulated climates at 1.5 °C predict simulated climates at 2 °C of global mean warming. While in many locations, the seasonal average was determined to be a useful predictor of change at higher levels of global warming,

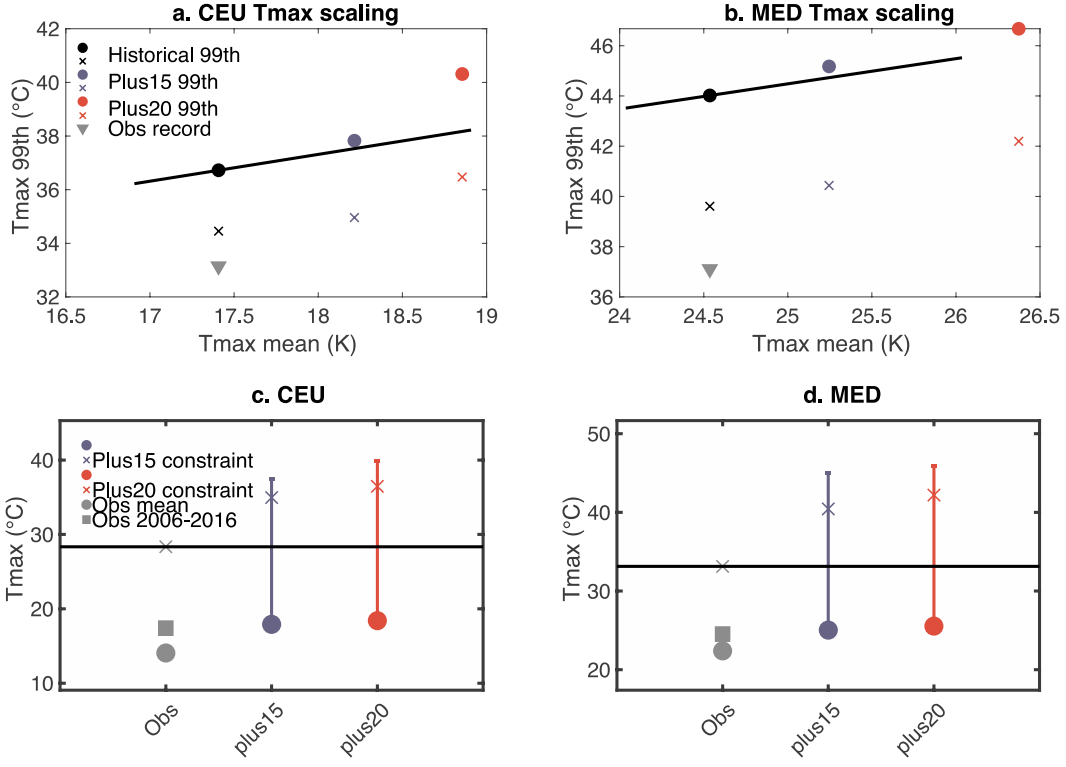

Fig. 8. Example of Tmax mean-99th percentile scaling between HAPPI experiments for (a) CEU (Central Europe) and (b) MED (Mediterranean). Ensemble mean Tmax and 99th percentile values are shown for both region for each experiment with circles ($HAPPI_{2006\text{-}2015}$ in black; $HAPPI1_{.5}$ in blue; $HAPPI_2$ in red). Crosses show the observational constraint ($HAPPI_{1.5/Obs}$ and $HAPPI_{2/Obs}$), indicating that values well above the observed constraint and current record (grey triangle) are simulated in HAPPI. Scaling lines are shown, demonstrating relationship if 99th percentile values increased at same rate as mean (1-1). The current observed record is shown (grey cross), in addition to the observed constraints on simulated values (blue and red crosses). Also shown (panel c and d) are assessments of simulated future extremes where simulated Plus15-Future (blue) and Plus20-Future (red) are adjusted based on observed mean temperatures and global mean warming levels. Observed mean values are shown in grey circle, and mean 2016–2016 observed values in grey circles. (For interpretation of the references to colour in this figure legend, the reader is referred to the Web version of this article.)

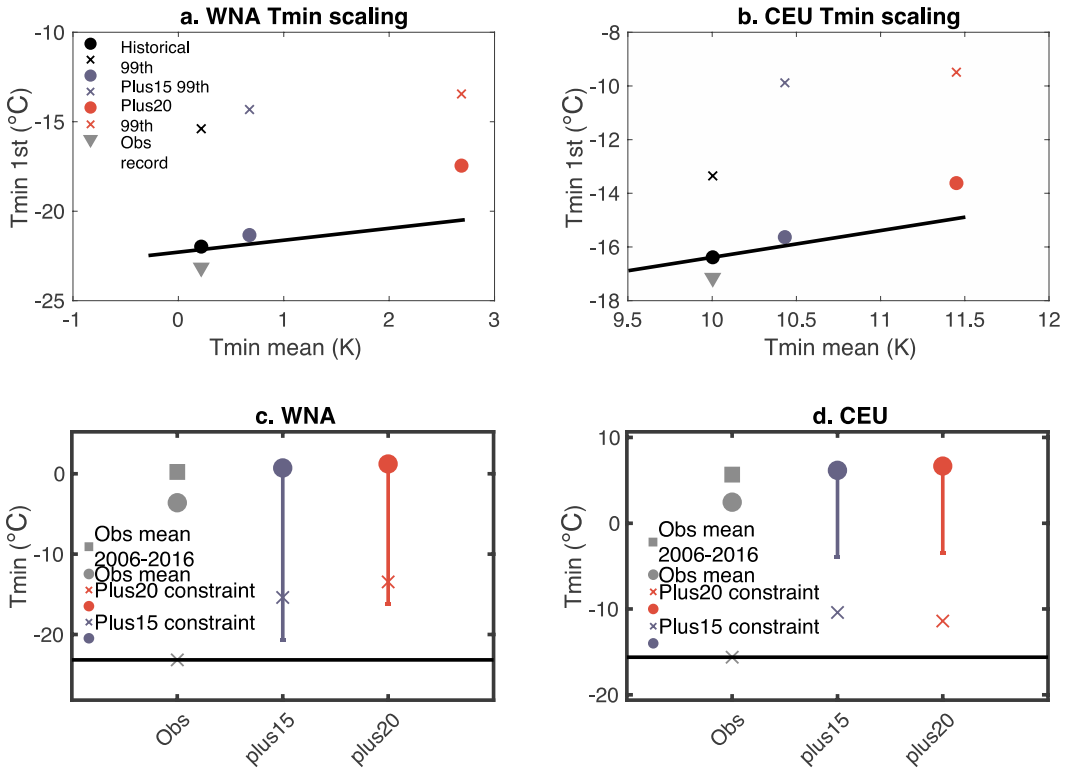

Fig. 9. As for Fig. 8, but showing Tmin mean-1st percentile scaling between HAPPI experiments for (a) WNA (Western North America) and (b) CEU (Central Europe). Ensemble mean Tmin and 1st percentile values for each region for each experiment are shown with circles ($HAPPI_{2006\text{-}2015}$ in black; $HAPPI1_{.5}$ in blue; $HAPPI_2$ in red). (For interpretation of the references to colour in this figure legend, the reader is referred to the Web version of this article.)

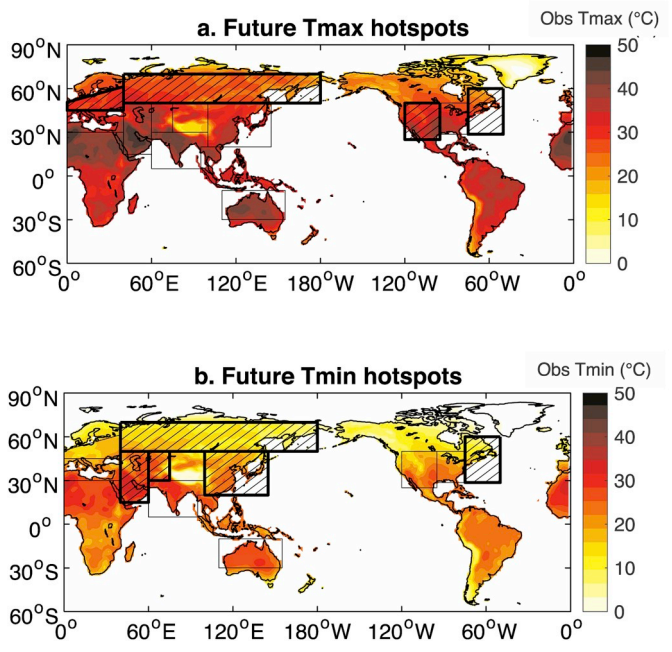

Fig. 10. Hotspots of future warming of Tmax (a) and Tmin (b). Hatched areas are regions where the tail of the temperature distribution (difference between 99th and 95th percentile/1st and 5th percentile values) expands more than mean temperatures between 1.5 °C and 2 °C of warming.

accelerated increased in extreme temperatures in the East Asian region were noted. In the King et al. (2018) investigation, temperature extremes increased between 1.5 °C and 2 °C levels of global mean warming, in part due to synoptic changes and changes in anthropogenic aerosol concentrations.

The location of hotspots of monthly temperature extremes determined in our current study also aligns well with previous studies, including the identification of East Asia as ahotspot of Tmax warming at 1.5 and 2 °C levels (Fig. 6). We note that the developing world regions around the tropics tended to fail the model evaluation tests we imposed, and we do not provide analysis of these regions, despite their established vulnerability to future climatic changes (Althor et al., 2016). The regions analysed in our study and determined to be hotspots of warming at largely mid-latitude areas, including the Mediterranean. The Mediterranean region has been previously identified as a regional climate change hotspot (Diffenbaugh and Giorgi, 2012; Seneviratne et al., 2016), and projections for increases in heatwave intensity here are the largest simulated globally (Perkins-Kirkpatrick and Gibson, 2017).

The Mediterranean region is highlighted as a hotspot of warming due to the strong soil moisture-temperature feedback that likely enhances changes in temperature extremes (Diffenbaugh et al., 2007; Seneviratne et al., 2006). Soil moisture conditions and feedbacks also have a notably large impact on the heatwave magnitude of heatwaves in central Europe (Bador et al., 2017; Vogel et al., 2018, 2017). At the specific individual extreme event level, such as the 2010 Russian heatwave and 2003 European heatwaves, heatwaves associated with blocking high pressure systems and soil-moisture feedbacks can amplify warming (Quesada et al., 2012; Miralles et al., 2014) and result temperature extremes of extended duration (Coumou et al., 2013; Bador et al., 2017). The overall magnitude of warming in 99th percentile regional monthly Tmax values determined in our study is at the higher end of values reported, though direct comparison across studies is difficult given the differing temperature metrics reported and different model experiments used. For example, one study found changes in heatwave intensity are 0.5–1.5 °C above a given global warming threshold (1.5 °C/2 °C), though values are higher over the Mediterranean (Perkins-Kirkpatrick and Gibson, 2017).

The high warming values determined in our study (up to 6 °C above

present for 1.5 °C of global mean warming) may result from several factors. First, Diffenbaugh et al. (2007) note that increases in temperature are highly sensitive to percentile analysed, and we use a comparatively more extreme temperature metric (99th rather than 95th percentile). This sensitivity to percentile is also demonstrated here in Fig. 4 (and Supplementary Figs. 5 and 6). In studies focused on record-breaking temperatures (e.g. the absolute highest values recorded), changes in the rates of record-breaking increase 5-fold (Coumou et al., 2013) or greater (King, 2017). Second, this very strong result for the Mediterranean may be caused by a combination of genuine sensitivity of extremes to mean temperature changes and additionally indicate that the 2006–2015 period used in the HAPPI modelling framework does not sufficiently constrain the tail of the distribution nor temperature variability in the extratropical Mediterranean location.

We have attempted to constrain the value of future warming in three case study regions (CEU and MED for Tmax; WNA and CEU for Tmin) using a large time slice-based ensemble, and by applying bias correction and observational constraints (Fig. 8c and d, Fig. 9 c and d). However, the values presented are based on a single modelling framework and hence a systematic examination of projections and uncertainties in a greater number and variety of models would assist in providing these projections of possible absolute regional temperature extremes under various levels of global mean warming. In particular, the estimation of variability simulated in models requires further examination.

While we have highlighted the MED and CEU regions, in particular, we note that many other regions analysed are classified as hotspots of warming for extreme monthly Tmax at 1.5 °C (CAS, EAS, NAS, SAS, WAS, CEU, MED, NAU) and/or 2 °C (EAS, SAS, CAS, CEU, MED, NAU, CAN, ENA) of global mean warming. In these listed regions, Tmax increases by more than the rate of warming of the global land surface. Processes such as land-atmosphere feedbacks (Seneviratne et al., 2010; Vogel et al., 2017) and/or dynamical changes (Wehrli et al., 2018) may be particularly important in these regions. For example, previous studies identify that land-atmosphere feedback in CEU amplify extreme temperatures in climate change projections (Vogel et al., 2017; Seneviratne and Coauthors, 2013). We also note that regions which are extremes hotspots of future Tmax warming (where the tails of the temperature distribution are most sensitive to global land surface warming) are not identical to Tmin hotspots. For example, NAU shows a greater sensitivity of Tmax to mean warming than for Tmin extremes. We label CEU, NAS, WNA and ENA as Tmax hotspots, and CAS, WAS, EAS, NAS, and ENA as Tmin hotspots.

In general, the proportionally large increase in extremes of temperature relative to global or regional temperature means is well established. One important result from this HAPPI analysis is that in many regions, the most extreme temperature percentiles analysed warmed at a faster rate with mean global warming level (e.g. 99th compared to 95th percentiles, see Fig. 8). We also show that this is regionally variable, and this relationship is also critically influenced by the mean global warming level, the temperature variable and extreme percentile considered. We summarise this complexity in mean-extreme relationships by describing overall hotspots of extreme warming, a description of regions that targets changes in the far tail of temperature distributions. Extreme temperatures in these regions, shown in Fig. 10 and Table 3, are most impacts by background changes in mean warming of the land surface. These results help to identify regions in which simple pattern scaling approaches may not be insightful about changes in regional extremes with increases in GLMT. Pattern scaling techniques may assist in approximating forced changes under increasing concentrations of greenhouse gases (Tebaldi and Arblaster, 2014). However, such scaling approaches are not universally applicable and can be model dependent. Further analysis demonstrates that for extremes of temperature, this assumption of linearity may not hold (Lustenberger et al., 2014).

The regional variability in responses of extremes to mean temperature changes is likely dependent on many factors, including forced responses in circulation, local- and regional-scale feedbacks and the degree of natural variability in temperatures. Exploring these dynamic processes and feedbacks, and their regional and seasonal variations in further detail would be useful. In particular decomposing changes in extremes into changes relating to mean warming and dynamically driven components would provide further insight into changes in these hotspot regions (Wehrli et al., 2018). Previous studies have also explored the role of antecedent rainfall or soil moisture in driving extreme high temperatures (Donat et al., 2018; Vogel et al., 2018). Donat et al. (2018) used the observed precipitation-hot temperature relationship as a constraint on projections of future temperature extremes. Such an approach could also be applied to simulations at varying levels of global mean warming, such as in HAPPI.

In our study, we restricted the analysis to HAPPI and explored temperatures only in multi-model ensembles. An exploration of potential inter- (between HAPPI models) and intra-model (between individual HAPPI model realisations) differences may provide insight into process-based understandings of warming of extremes. In particular, the relationship between precipitation and temperatures in models may elucidate strong Mediterranean region warming.

5. Conclusions

Overall, this study confirms the outcomes of prior studies that investigate the changing probability of current extreme temperatures under 1.5 °C and 2 °C of warming in transient model simulations, and demonstrate the overall benefits of limiting warming for reducing the frequency of future regional extreme temperatures (Ciavarella et al., 2017). By estimating absolute temperature extremes under Paris Agreement higher global mean warming levels in stabilised model simulations, we provide additional information about the regions in which changes in extremes are greatest relative to changes in mean temperatures, and the severity of such changes in temperature extremes under the Paris Agreement temperature thresholds.

We find that under both Paris Agreement levels of warming, increases in 99th percentile monthly Tmax values are projected for all regions, although these projections are regionally variable and values of these Tmax extremes do not increase 1-1 with global mean warming in many regions. We find many mid-latitude regions where extremes of Tmax (99th percentile) and Tmin (1st percentile) values increase more than average warming of the global land surface (the 1:1 warming line shown in Figs. 4, 5, 8 and 9), although the designation of these regions as hotspots depends on the temperature variable (Tmin or Tmax), percentile and global mean warming level considered. We define hotspots of extremes as regions in which the tail of the temperature distribution (above 99th percentile) increases with mean land surface warming at a faster rate than the rest of the temperature distribution. For Tmax, CEU, NAS, WAS and ENA experience the greatest projected increases in extremes relative to means, and for Tmin CAS, WAS, EAS, NAS and ENA are identified as extremes hotspots. Prior studies have also found that regional extreme temperatures increase with global mean temperatures, but with a slope greater than 1 (Seneviratne et al., 2016).

These results using different temperature parameters (99th percentile values) and model frameworks re-iterate that while global mean warming provides a useful and necessary metric for examining large-scale climate changes and for policy discussions, this single metric does not sufficiently reveal changes in regional temperature across the spectrum of the temperature distribution. In some regions, changes in extremes are highly sensitive to and far exceed changes in global means. For example, we show projections for changes in Tmax extremes in the Mediterranean region that are up to 6 °C above present for 1.5 °C of global mean warming. While this specific result requires further process-based exploration and analysis in an expanded set of models, it further demonstrates the necessity for exploring projected changes in regional-scale temperature extremes.

Declaration of Competing Interest

None.

Acknowledgements

We acknowledge the support of the NCI facility in Australia. S.C.L is funded through the Australian Research Council (DE160100092). S.E. P.-K. is funded through the Australian Research Council (FT170100106). A.D.K. is funded through the Australian Research Council (DE180100638). DMM is funded by a NERC fellowship (NE/N014057/1).

Appendix A. Supplementary data

Supplementary data to this article can be found online at https://doi.org/10.1016/j.wace.2019.100233.

References

Alexander, L., Coauthors, 2006. Global observed changes in daily climate extremes of temperature and precipitation. J. Geophys. Res. Atmos. 111 https://doi.org/10.1029/2005JD006290.

Althor, G., Watson, J.E.M., Fuller, R.A., 2016. Global mismatch between greenhouse gas emissions and the burden of climate change. Sci. Rep. 6, 1–6. https://doi.org/10.1038/srep20281.

Bador, M., Terray, L., Boé, J., Somot, S., Alias, A., Gibelin, A.L., Dubuisson, B., 2017. Future summer mega-heatwave and record-breaking temperatures in a warmer France climate. Environ. Res. Lett. 12 https://doi.org/10.1088/1748-9326/aa751c.

Ciavarella, A., Stott, P., Lowe, J., 2017. Early benefits of mitigation in risk of regional climate extremes. Nat. Clim. Chang. 7, 326–330. https://doi.org/10.1038/nclimate3259.

Coumou, D., Robinson, A., 2013. Historic and future increase in the global land area affected by monthly heat extremes. Environ. Res. Lett. 8, 3–8. https://doi.org/10.1088/1748-9326/8/3/034018.

Coumou, D., Robinson, A., Rahmstorf, S., 2013. Global increase in record-breaking monthly-mean temperatures. Clim. Change 118, 771–782. https://doi.org/10.1007/s10584-012-0668-1.

Diffenbaugh, N.S., Giorgi, F., 2012. Climate change hotspots in the CMIP5 global climate model ensemble. Clim. Change 114, 813–822. https://doi.org/10.1007/s10584-012-0570-x.

Diffenbaugh, N.S., Pal, J.S., Giorgi, F., Gao, X., 2007. Heat stress intensification in the Mediterranean climate change hotspot. Geophys. Res. Lett. 34, 1–6. https://doi.org/10.1029/2007GL030000.

Diffenbaugh, N.S., Singh, D., Mankin, J.S., 2018. Unprecedented climate events: historical changes, aspirational targets, and national commitments. Sci. Adv. 4, 1–10. https://doi.org/10.1126/sciadv.aao3354.

Donat, M.G., Pitman, A.J., Angélil, O., 2018. Understanding and reducing future uncertainty in midlatitude daily heat extremes via land surface feedback constraints. Geophys. Res. Lett. 45 (10), 636. https://doi.org/10.1029/2018GL079128, 627-10.

Dosio, A., Mentaschi, L., Fischer, E.M., King, A.D., Karoly, D.J., 2017. Climate Extremes in Europe at 1 . 5 and 2 Degrees of Global Warming Climate Extremes in Europe at 1 . 5 and 2 Degrees of Global Warming.

Fischer, E.M., Beyerle, U., Schleussner, C.F., King, A.D., Knutti, R., 2018. Biased estimates of changes in climate extremes from prescribed SST simulations. Geophys. Res. Lett. 45, 8500–8509. https://doi.org/10.1029/2018GL079176.

Hansen, J., Sato, M., Ruedy, R., 2012. Perception of climate change. Proc. Natl. Acad. Sci. 109, E2415–E2423. https://doi.org/10.1073/pnas.1205276109.

Harris, I., Jones, P.D., Osborn, T.J., Lister, D.H., 2014. Updated high-resolution grids of monthly climatic observations - the CRU TS3.10 Dataset. Int. J. Climatol. 34, 623–642. https://doi.org/10.1002/joc.3711.

Haustein, K., Allen, M.R., Forster, P.M., Otto, F.E.L., Mitchell, D.M., Matthews, H.D., Frame, D.J., 2017. A real-time global warming index. Sci. Rep. 7, 1–6. https://doi.org/10.1038/s41598-017-14828-5.

He, J., Soden, B.J., 2016. The impact of SST biases on projections of anthropogenic climate change: a greater role for atmosphere-only models? Geophys. Res. Lett. 43, 7745–7750. https://doi.org/10.1002/2016GL069803.

Herger, N., Sanderson, B.M., Knutti, R., 2015. Improved pattern scaling approaches for the use in climate impact studies Supplementary Information. Geophys. Res. Lett. 42, 3486–3494. https://doi.org/10.1002/2015GL063569.

IPCC, 2012. Managing the risks of extreme events and disasters to advance climate change adaptation. In: A Special Report of Working Groups I and II of the Intergovernmental Panel on Climate Change. Cambridge University Press, 582 pp.

James, R., Washington, R., Schleussner, C.F., Rogelj, J., Conway, D., 2017. Characterizing half-a-degree difference: a review of methods for identifying regional climate responses to global warming targets. Wiley Interdiscip. Rev. Clim. Chang. 8 https://doi.org/10.1002/wcc.457.

Karmalkar, A.V., Bradley, R.S., 2017. Consequences of global warming of 1.5 °c and 2 °c for regional temperature and precipitation changes in the contiguous United States. PLoS One 12, 1–17. https://doi.org/10.1371/journal.pone.0168697.

Kharin, V.V., Flato, G.M., Zhang, X., Gillett, N.P., Zwiers, F., Anderson, K.J., 2018. Risks from climate extremes change differently from 1.5°C to 2.0°C depending on rarity. Earth's Futur. https://doi.org/10.1002/2018EF000813.

King, A.D., 2017. Attributing changing rates of temperature record breaking to anthropogenic influences. Earth's Futur 5, 1156–1168. https://doi.org/10.1002/2017EF000611.

King, A.D., 2019. The drivers of nonlinear local temperature change under global warming. Environ. Res. Lett. 14, 064005 https://doi.org/10.1088/1748-9326/ab1976.

King, A.D., Black, M.T., Min, S.K., Fischer, E.M., Mitchell, D.M., Harrington, L.J., Perkins-Kirkpatrick, S.E., 2016. Emergence of heat extremes attributable to anthropogenic influences. Geophys. Res. Lett. 43, 3438–3443. https://doi.org/10.1002/2015GL067448.

King, A.D., Karoly, D.J., Henley, B.J., 2017. Australian climate extremes at 1.5 °c and 2 °c of global warming. Nat. Clim. Chang. 7, 412–416. https://doi.org/10.1038/nclimate3296.

King, A.D., Knutti, R., Uhe, P., Mitchell, D.M., Lewis, S.C., Arblaster, J.M., Freychet, N., 2018. On the linearity of local and regional temperature changes from 1.5°C to 2°C of global warming. *J. Clim.*, JCLI-D-17-0649.1. https://doi.org/10.1175/JCLI-D-17-0649.1.

Lewis, S.C., King, A.D., Mitchell, D.M., 2017. Australia's unprecedented future temperature extremes under Paris limits to warming. Geophys. Res. Lett. 44, 9947–9956. https://doi.org/10.1002/2017GL074612.

Lustenberger, A., Knutti, R., Fischer, E.M., 2014. The potential of pattern scaling for projecting temperature-related extreme indices. Int. J. Climatol. 34, 18–26. https://doi.org/10.1002/joc.3659.

Miralles, D.G., Teuling, A.J., Van Heerwaarden, C.C., De Arellano, J.V.G., 2014. Mega-heatwave temperatures due to combined soil desiccation and atmospheric heat accumulation. Nat. Geosci. https://doi.org/10.1038/ngeo2141.

Mitchell, D., James, R., Forster, P.M., Betts, R.A., Shiogama, H., Allen, M., 2016. Realizing the impacts of a 1.5 °C warmer world. Nat. Clim. Chang. 6, 735–737. https://doi.org/10.1038/nclimate3055.

Mitchell, D., Coauthors, 2017. Half a degree additional warming, prognosis and projected impacts (HAPPI): background and experimental design. Geosci. Model Dev. (GMD) 10, 571–583. https://doi.org/10.5194/gmd-10-571-2017.

Nangombe, S., Zhou, T., Zhang, W., Wu, B., Hu, S., Zou, L., Li, D., 2018. Record-breaking climate extremes in Africa under stabilized 1.5 °c and 2 °c global warming scenarios. Nat. Clim. Chang. 8, 375–380. https://doi.org/10.1038/s41558-018-0145-6.

Perkins-Kirkpatrick, S.E., Gibson, P.B., 2017. Changes in regional heatwave characteristics as a function of increasing global temperature. Sci. Rep. 7, 1–12. https://doi.org/10.1038/s41598-017-12520-2.

Perkins, S.E., 2015. A review on the scientific understanding of heatwaves-Their measurement, driving mechanisms, and changes at the global scale. Atmos. Res. 164–165, 242–267. https://doi.org/10.1016/j.atmosres.2015.05.014.

Quesada, B., Vautard, R., Yiou, P., Hirschi, M., Seneviratne, S.I., 2012. Asymmetric European summer heat predictability from wet and dry southern winters and springs. Nat. Clim. Chang. https://doi.org/10.1038/nclimate1536.

Rohde, R., Coauthors, 2013. A New Estimate of the Average Earth Surface Land Temperature Spanning 1753 to 2011, vol. 01. Geoinformatics Geostatistics An Overv, pp. 1–7. https://doi.org/10.4172/2327-4581.1000101.

Seneviratne, S.I., Lüthi, D., Litschi, M., Schär, C., 2006. Land-atmosphere coupling and climate change in Europe. Nature 443, 205–209. https://doi.org/10.1038/nature05095.

Seneviratne, S.I., Corti, T., Davin, E.L., Hirschi, M., Jaeger, E.B., Lehner, I., Orlowsky, B., Teuling, A.J., 2010. Investigating soil moisture-climate interactions in a changing climate: a review. Earth Sci. Rev. https://doi.org/10.1016/j.earscirev.2010.02.004.

Seneviratne, S.I., Coauthors, 2013. Impact of soil moisture-climate feedbacks on CMIP5 projections: first results from the GLACE-CMIP5 experiment. Geophys. Res. Lett. https://doi.org/10.1002/grl.50956.

Seneviratne, S.I., Donat, M.G., Pitman, A.J., Knutti, R., Wilby, R.L., 2016. Allowable CO2 emissions based on regional and impact-related climate targets. Nature 529, 477–483. https://doi.org/10.1038/nature16542.

Taylor, K.E., Stouffer, R.J., Meehl, G.A., 2012. An overview of CMIP5 and the experiment design. Bull. Am. Meteorol. Soc. 93, 485–498. https://doi.org/10.1175/BAMS-D-11-00094.1.

Tebaldi, C., Arblaster, J.M., 2014. Pattern scaling: its strengths and limitations, and an update on the latest model simulations. Clim. Change 122, 459–471. https://doi.org/10.1007/s10584-013-1032-9.

Tebaldi, C., Knutti, R., 2018. Evaluating the accuracy of climate change pattern emulation for low warming targets. Environ. Res. Lett. 13 https://doi.org/10.1088/1748-9326/aabef2.

UNFCCC, 2016. Paris agreement. Article 2, 1–27.

Vogel, M.M., Orth, R., Cheruy, F., Hagemann, S., Lorenz, R., van den Hurk, B.J.J.M., Seneviratne, S.I., 2017. Regional amplification of projected changes in extreme temperatures strongly controlled by soil moisture-temperature feedbacks. Geophys. Res. Lett. https://doi.org/10.1002/2016GL071235.

Vogel, M.M., Zscheischler, J., Seneviratne, S.I., 2018. Varying soil moisture–atmosphere feedbacks explain divergent temperature extremes and precipitation projections in central Europe. Earth Syst. Dyn. 9, 1107–1125. https://doi.org/10.5194/esd-9-1107-2018.

Wang, Z., Lin, L., Zhang, X., Zhang, H., Liu, L., Xu, Y., 2017. Scenario dependence of future changes in climate extremes under 1.5 °c and 2 °c global warming. Sci. Rep. 7, 1–9. https://doi.org/10.1038/srep46432.

Wehrli, K., Guillod, B.P., Hauser, M., Leclair, M., Seneviratne, S.I., 2018. Assessing the dynamic versus thermodynamic origin of climate model biases. Geophys. Res. Lett. https://doi.org/10.1029/2018GL079220.

Zappa, G., Shepherd, T.G., 2017. Storylines of atmospheric circulation change for European regional climate impact assessment. J. Clim. 30, 6561–6577. https://doi.org/10.1175/JCLI-D-16-0807.1.